PANAMGEO CHILE 2024
17th PAN-AMERICAN CONFERENCE ON SOIL MECHANICS AND GEOTECHNICAL ENGINEERING | 2nd LATIN-AMERICAN REGIONAL CONFERENCE OF IAEG
LA SERENA • CHILE / NOVEMBER 12 - 16, 2024

Proceedings of the 17th Pan-American Conference on Soil Mechanics and Geotechnical Engineering (XVII PCSMGE), and 2nd Latin-American Regional Conference of the International Association for Engineering Geology and the Environment (IAEG), La Serena Chile, 2024.

Oedometric continuous corrected law for settlements estimate on shallow foundations.

Aplicación de la ley edométrica continua corregida para la estimación de asentamientos en fundaciones poco profundas.

Wagdi Naime
Civil Engineering School, Central University of Venezuela, Venezuela, wagdin@gmail.com

ABSTRACT: The oedometric continuous law is an alternative to the conventional law currently used to interpret oedometric behavior. This new law is better adapted to the experimental results than the conventional method, shown through published results with analysis of several oedometric tests on soils, ranging from low to high compressibility. Considering stress paths starting from the ko line, of the oedometric behavior, tending towards the stress limit state line, is defined a new stress-strain law that better fits real behavior under shallow foundations, called oedometric continuous corrected law. This new method allows effective analysis of the soil deformations under shallow foundations with accurate estimates of settlement, vertical deformations, and lateral displacement profiles. This paper shows 32 historical cases of measured and calculated settlements using the oedometric continuous corrected law against the results obtained by using the oedometric criterion. The results show a better adaptation of this new law with the measured settlements making it better suited for settlements estimates on shallow foundations.

KEYWORDS: Compressibility, oedometric strain, horizontal deformation, settlements of shallow foundations, stress path.

1 INTRODUCTION

For almost a century the conventional oedometric method has been widely used primarily on consolidation settlements estimates on shallow foundations (e. g.: Balasubramaniam et al., 2010; Chen et al., 2019; Indraratna et al., 2017; Peck, 1955; Skempton et al., 1955; Wijemunige & Moh, 1989; Yune & Olgun, 2016). The oedometric criterion does not take into account the horizontal deformations, although it is worth mentioning that below shallow foundations the soil presents horizontal deformations, which have been proven by real-scale load tests (Briaud & Gibbens, 1997, 1999; Da Fonseca et al., 1997; Eggestad, 1964; Loganathan et al., 1993; Wijemunige & Moh, 1989). Then for the normal design conditions, comparing the oedometric settlement calculations with the real measured values, we can note that the oedometric criterion underestimates the settlement with differences ranging between 13% and 22% (Chen et al., 2019; Naime, 2019; Peck, 1955; Skempton et al., 1955).

The conventional oedometric law is based on the recompression and the compression indexes (Cr and Cc), which are the assumed straight-line slopes on the two first zones of the e-log(σ) compressibility curve. The e-log(σ) curve is highly nonlinear and it is not appropriate to be defined by simple Cr and Cc values. If we assume that Cc and Cr are constants, then we will obtain the non-continuous equations on the precompression pressure σm. Published experimental results reveal that the compressibility equations could be curved and continuous. Sridharan & Gurtug (2005) show a clear variation of the slope Cci in the compressibility curve versus axial pressure. Mesri & Choi (1985) proposed a modified compression index C´c, which is the slope of the lines connecting the σm point and several points on the compressibility curve.

Naime (2019) proposed a nonlinear and continuous oedometric criterion, called the oedometric-continuous law, which defines a high correlation on both, the pre-consolidated and normally consolidated domains of the compressibility curve and the oedometric stress-strain relationship. This new law is supported by the analysis of the oedometric modulus variation versus effective axial stress, suggested previously by several researchers (Janbu, 1963; Ohde, 1939; Papadopoulos, 1992; Stamatopoulos & Kotzias, 1974, 1978; Wissa et al., 1971). The continuous equations were developed based on the hypothesis that the oedometric modulus increases linearly with the effective axial stress starting from an initial value (Eso > 0), with constant slope λ. Moreover, the analysis of several oedometric tests on soils ranging from low to high compressibility, has shown that the oedometric-continuous law is better adapted to the experimental results than the conventional method (Naime, 2019, 2022).

The oedometric-continuous equations can be derived from the practical application domain, making it possible to be used in advanced numerical simulations which are ideal for superimposing effects that complement the oedometric behaviour, e.g., the effects of the horizontal deformations. Naime (2022) and Naime & Gavidia (2022b, 2022a), show the modification of the stress-strain equation to the continuous oedometric law, including the horizontal deformations effect. The oedometric-continuous corrected law, that superimposes the horizontal deformations effect on the vertical oedometric deformation, allows an effective analysis of soil stresses and deformations under shallow

foundations with accurate estimates of the vertical deformations, lateral displacement profiles and the failure zones.

This research presents the application of this new law in settlement estimates under shallow foundations through 32 historical cases of measured and calculated settlements using the oedometric continuous corrected law against the results obtained by using the oedometric criterion method.

2 STRESS-STRAIN RELATIONSHIP FOR THE OEDOMETRIC CONTINUOUS CORRECTED LAW

The stress-strain relationship for the oedometric continuous corrected law (Eq. 1) has been development in Naime (2022). The fundamental bases are: the stress paths starting from the ko line, of the oedometric behavior, tending towards the kf line, of the stress limit state (Figure 1), and a parabolic function scaling on the horizontal strains in the extension zone (Figure 2). There is a gradual reduction in the horizontal stress compared to the horizontal stress in the oedometric condition.

$$\varepsilon_z = \frac{1}{\lambda}\ln\left[1+\frac{\lambda\Delta\sigma_z}{E_{so}+\lambda\sigma_{oz}}\right] + 2\varepsilon_{h_f}\left(\sqrt{1-\frac{\Delta\sigma_z}{\sigma_{z_f}-\sigma_{oz}}}-1\right) \quad (1)$$

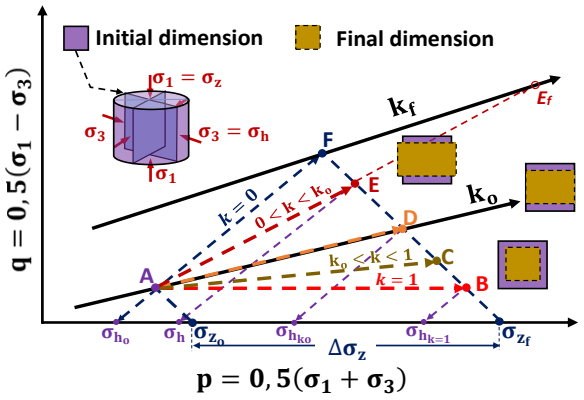

Figure 1. Theoretical correlations among stress path with axisymmetric conditions and lateral deformations on the soil (Naime, 2022).

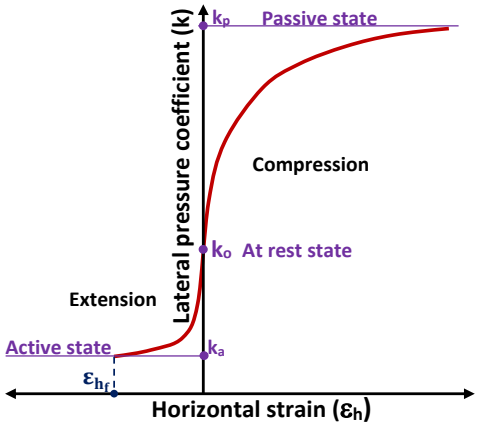

Figure 2. Theoretical graphical relationship between horizontal strain and the lateral pressure coefficient (Naime, 2022).

These stress paths represent a vertical stress increase $\Delta\sigma_z$ starting from vertical and horizontal initial stresses σ_{z_o} and σ_{h_o}. The horizontal deformation is conditioned by the final horizontal stress: at the right-hand side of $\sigma_{h_{ko}}$ a compression will form and at the left-hand side will get an extension. Under a shallow foundation, the final horizontal stress σ_h will be between σ_{h_o} and $\sigma_{h_{ko}}$ just as the A→E path, could be projected to failure at the point E_f as $\Delta\sigma z$ increases.

In the relationship between the horizontal deformation and the coefficient of the lateral pressure (k), the extension path is assumed equivalent to a parabolic curve. Thus, equation 2 presents the horizontal deformation varying from the initial rest state ($\varepsilon h = 0$) to the horizontal deformation at failure (εhf) while k is reduced from ko to ka.

$$\frac{\varepsilon_h}{\varepsilon_{h_f}} = \sqrt{1-\frac{k_o-k}{k_o-k_a}} - 1 \quad (2)$$

The final horizontal stress has an intermediate value between σ_{h_o} and $\sigma_{h_{ko}}$ (Eq. 3). The η value pin points the horizontal stress to be between the indicated limits. If $\eta = ½$, σ_h is the midpoint, $\eta = 0$ or $\eta = 1$ represent either the conditions of the shearing stage of a consolidate-drained test or the oedometric test respectively (σ_h is σ_{h_o} or $\sigma_{h_{ko}}$).

$$\sigma_h = k_o(\sigma_{z_o} + \eta\Delta\sigma_z) \quad (3)$$

For the stress-strain relationship, according to Eq. 1, for any depth (*z*), ε_z is the vertical strain, $\Delta\sigma_z$ is the vertical effective stress increment, σ_{zo} is the initial vertical effective stress, ε_{hf} is the horizontal strain at failure, σ_z is the final vertical effective stress and σ_{zf} is the effective vertical stress that produces the failure depending to the respective stress path (or η value), according to the Mohr-Coulomb criterion. Figure 3 shows an application of this equation. The curve determined with the stress path obtained by the elasticity equations is also present, representing theoretically the stress path method (Lambe & Marr 1979).

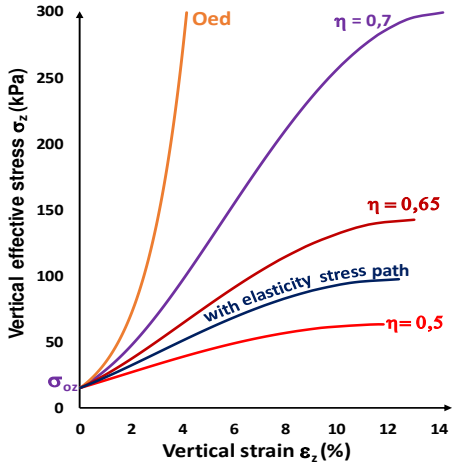

Figure 3. Vertical stress–strain relationship by the oedometric-continuous corrected law. Guayana City's silty clay at z= 0.75 m depth (Naime, 2022).

The influence of the roughness on the soil-foundation contact is treated as an additional increase of the horizontal confinement stress. This reduces the horizontal deformations obtained by Eq. 3 and consequently increases the vertical effective stress at failure σ_{zf}. At the soil-foundation contact the induced horizontal stress is large and decreases with depth. Using a constant η value, the stress paths at different depths are not parallel and have a higher inclination as depth increases, due to the scarce increment in the horizontal stress resulting from roughness. The proposed procedure includes the roughness effect on deformations, and on the bearing capacity of shallow foundations (Naime 2022). The settlement is calculated through the integration of Eq. 1 with respect to depth. Elastic solutions, like Bousinesq equation, are used to determine the vertical stress increment Δσz

3 MATERIALS AND METHOD

We have considered 32 cases of measured and calculated settlements in shallow foundations obtained from several references in the technical literature and analyzed using the corrected continuous oedometric equation, among these references we can mention: Peck (1955) and Skempton et al. (1955): the Fire Testing Station of London, the Chelsea Bridge of London, the Waterloo Bridge of London, the Masonic Temple of Chicago (7 cases), the Monadnock Block of Chicago (3 cases), Auditorium Tower of Chicago (3 cases), the Apartment Building on Chicago (3 cases); Chen et al. (2019): the Shanghai Theme Park (12 cases) and Balasubramaniam et al. (2007) and Wijemunige & Moh (1989): one embankment on Muar clay, Malaysia.

The parameters of the oedometric-continuous model (λ and Eso), were obtained by back calculating methods, based on the compressibility parameters considered in the original references. The same conditions and soil profiles presented in the original references were reproduced for the settlement's calculation.

If the compressibility curve is known, E_{so} and λ are determined directly from this curve. If only the compressibility parameters of the conventional law are known, such as the compressibility modulus m_v or the recompression and compression indices, back-calculation is performed, so that the settlement calculations, using the conventional law or the continuous oedometric law, considering the original conditions of each case, are equivalent. In each case, the field compressibility curves, based on the conventional parameters, are reproduced and compared with the one based on the continuous law.

Table 1 presents these main characteristics. The strength parameters and the horizontal deformation at failure for each soil were obtained by the original information or by reference of another similar soils. The oedometric settlement estimates were obtained from each original reference. Numerical methods were used to integrate the Eq. 1, applying the Romberg method (R9). The horizontal stress factor used was η = 0.5.

The settlement is estimated through the integration of the Eq. 1:

$$S_t = \int_{z_i}^{z_f} \left[\frac{1}{\lambda} ln\left(1 + \frac{\lambda \Delta\sigma_z}{E_{so} + \lambda\sigma_{oz}}\right) + 2\varepsilon_{h_f}\left(1 - \sqrt{1 - \frac{\Delta\sigma_z}{\sigma_{z_{falla}} - \sigma_{oz}}}\right)\right] dz \quad (4)$$

Equation 4 is separated into two integrals (Eq. 5), the first for the oedometric settlement, and the second to estimate the increase in settlement due to the effects of horizontal deformations (Eq. 6).

$$S_t = S_{T_{oed}} + \Delta S_T \quad (5)$$

$$\Delta S_T = 2\varepsilon_{h_f} \int_{z_i}^{z_i} \left(1 - \sqrt{1 - \frac{\Delta\sigma_z}{\sigma_{z_{falla}} - \sigma_{oz}}}\right) dz \quad (6)$$

4 RESULTS AND DISCUSSION

Table 2 shows the measured settlements, the estimation by the oedometric criterion (OC) and the settlements calculated through the oedometric continuous corrected law (OCCL). Additionally, the types of foundations and the main geometric data are shown, as well as the water table and the contact pressure. Figure 4 shows the fit comparison of the oedometric criterion and the oedometric continuous corrected law with the measured settlements.

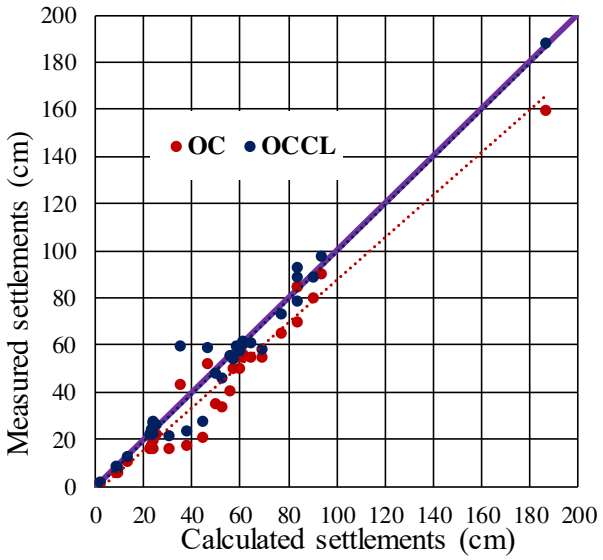

Figure 4. Fit comparison of the oedometric criterion (OC) and the oedometric continuous corrected law (OCCL) with the measured settlements.

The oedometric criterion, as previously indicated, underestimated the real settlements with an average $S_{calc}/S_{measured}$ ratio of 86.4% in these 32 cases, where the results were grouped around a line of lesser inclination than the 45º line.

The oedometric continuous corrected law shows results clustered around the 45º line, with an average $S_{calc}/S_{measured}$ ratio of 101.4%.

.

Table 1. Stratigraphic profiles description.

Place	Profile		H	Compressibility parameters					Strength parameters		
			m	m_v kPa^{-1}	Cc	Cr	e_o	E_{so} kPa	λ	ϕ °	C kPa	ε_{hf} %
Fire Testing Station, London		Brown London clay	6,10	1,61E-04	-	-	-	2676,67	62,31	29	40,00	3,0
Chelsea Bridge, London		Blue London clay	18,29	7,10E-05	-	-	-	7790,00	33,00	26	30,00	4,0
Waterloo Bridge, London		Blue London clay	12,19	8,52E-05	-	-	-	6436,93	29,91	26	30,00	4,0
Masonic Temple, Chicago	E1	Stiff SoilE12:E41	0,76	Assumed incompressible								
	E2	Medium soft Chicago clay	1,52	-	0,294	-	0,812	300,90	11,61	28	30	5,0
	E3	Medium soft Chicago clay	1,52	-	0,294	-	0,812	342,41	11,47	28	35	5,0
	E4	Medium soft Chicago clay	1,52	-	0,294	-	0,812	399,22	11,31	28	35	5,0
	E5	Medium soft Chicago clay	1,52	-	0,294	-	0,812	445,41	11,22	28	40	5,0
	E6	Medium soft Chicago clay	2,82	-	0,221	-	0,672	625,74	13,74	29	45	4,0
	E7	Medium soft Chicago clay	2,82	-	0,221	-	0,672	719,50	13,81	29	50	4,0
Manadnock Block, Chicago	E1	Stiff soil	1,37	Assumed incompressible								
	E2	Soft Chicago clay	1,83	-	0,263	-	0,756	327,67	13,21	24	38	5,1
	E3	Soft Chicago clay	1,83	-	0,263	-	0,756	387,32	13,07	24	39	4,9
	E4	Medium soft Chicago clay	2,36	-	0,207	-	0,644	547,30	15,26	25	42	4,0
	E5	Medium soft Chicago clay	2,36	-	0,207	-	0,644	645,63	15,00	25	44	3,7
	E6	Medium soft Chicago clay	2,36	-	0,207	-	0,644	737,62	14,87	25	45	3,3
	E7	Medium soft Chicago clay	2,36	-	0,207	-	0,644	824,06	14,83	25	46	3,0
Chicago Auditorium	E1	Medium soft Chicago clay	0,91	-	0,294	-	0,812	305,61	11,48	24	36	5,6
	E2	Soft Chicago clay	3,66	-	0,405	-	1,008	302,96	9,15	24	36	5,8
	E3	Soft Chicago clay	1,22	-	0,582	-	1,260	280,78	7,17	24	35	6,0
	E4	Medium soft Chicago clay	3,66	-	0,221	-	0,672	626,73	14,03	25	41	4,2
	E5	Medium soft Chicago clay	3,66	-	0,221	-	0,672	748,43	14,11	25	43	3,8
	E6	Stiff Chicago clay	3,35	-	0,106	-	0,406	1523,87	24,87	28	68	3,0
	E7	Stiff Chicago clay	4,27	-	0,079	-	0,336	2255,10	31,93	32	100	3,0
Apartament Building, Chicago	E1	Stiff Soil	1,22	Assumed incompressible								
	E2	Soft Chicago clay	1,52	-	0,277	-	0,784	335,77	12,40	24	37	5,5
	E3	Soft Chicago clay	1,52	-	0,277	-	0,784	382,44	12,35	24	37	5,3
	E4	Soft Chicago clay	1,52	-	0,277	-	0,784	430,19	12,24	24	38	5,2
	E5	Medium soft Chicago clay	3,20	-	0,180	-	0,588	696,72	16,56	25	44	3,6
	E6	Medium soft Chicago clay	3,20	-	0,180	-	0,588	838,18	16,43	25	46	3,1
Shanghai Theme Park	E1	Soft silty clay (S2)	3,00	-	0,320	-	1,100	300,62	10,56	24	25,0	3,0
	E2	Soft Shanghai clay (S3)	6,00	-	0,570	-	1,400	401,80	6,41	25	20,0	3,0
	E3	Soft Shanghai clay (S4)	0 - 7,5	-	0,430	-	1,200	581,21	7,78	25	25,0	3,0
Large-scale field trial embankment, Malaysia	E1	Weathered Muar clay	2,00	-	0,500	0,200	1,600	2000,00	15,00	12	8,00	7,0
	E2	Very soft silty Muar clay	6,00	-	1,500	0,200	2,600	280,00	1,50	10	10,00	7,0
	E3	Soft silty Muar clay	8,00	-	0,750	0,200	1,600	1700,00	10,00	17	18,00	7,0

Table 2. Measured and calculated settlements.

	Case	Type of Foundation	D_f	BxL	h_w	q	Settlements (cm)		
			m	m	m	kPa	Measured	OC	OCCL
1	Fire Testing Station, London	Isolated spread footing	-2,134	1,52x3,05	-0,61	84,48	1,7	1,5	1,7
2	Chelsea Bridge, London	Isolated spread footing	-9,449	8,53x32,31	3,96	179,51	8,4	5,6	8,2
3	Waterloo Bridge, London	Isolated spread footing	-6,706	8,23x35,66	5,18	263,98	13,2	10,7	12,9
4	Masonic Temple, Chicago	Mat footing	-4,267	38,10x55,47	-3,05	70,75	24,9	22,4	26,0
5	Masonic Temple, Chicago (Column 1)	Isolated spread footing	-4,267	4,88x5,18	-3,05	150,81	22,2	16,2	21,9
6	Masonic Temple, Chicago (Column 26)	Isolated spread footing	-4,267	4,88x5,18	-3,05	153,51	23,5	16,3	22,1
7	Masonic Temple, Chicago (Column 8)	Isolated spread footing	-4,267	4,88x5,18	-3,05	166,19	23,0	17,7	24,0
8	Masonic Temple, Chicago (Column 69)	Isolated spread footing	-4,267	6,10x7,01	-3,05	164,29	23,5	20,2	27,5
9	Masonic Temple, Chicago (Column 70)	Isolated spread footing	-4,267	6,10x7,01	-3,05	158,61	24,0	19,6	26,7
10	Masonic Temple, Chicago (Column 19)	Isolated spread footing	-4,267	4,88x5,18	-3,05	148,55	30,5	16,0	21,6
11	Monadnock Block, Chicago	Mat footing	-3,810	26,82x64,62	-3,05	116,15	55,9	40,6	55,4
12	Manadnock Block, Chicago (d-plate)	Combined footing	-3,810	7,16x8,99	-3,05	172,85	49,9	35,1	47,9
13	Manadnock Block, Chicago (e-plate)	Combined footing	-3,810	7,16x8,99	-3,05	164,52	52,5	33,8	46,1
14	Chicago Auditorium	Mat footing	-5,182	20,42x30,48	-3,05	120,38	61,0	55,9	60,2
15	Chicago Auditorium (k-m-p points)	Isolated spread footing	-5,182	3,05x3,05	-3,05	123,34	9,0	5,6	7,7
16	Chicago Auditorium (d point)	Mat footing	-5,182	20,42x30,48	-3,05	124,34	46,6	52,0	59,2
17	Apartament Building, Chicago (a-plate)	Mat footing section	-4,267	5,64x6,10	-3,35	230,78	37,8	17,6	23,6
18	Apartament Building, Chicago (g-plate)	Mat footing section	-4,267	5,64x6,10	-3,35	276,94	44,4	20,5	27,6
19	Apartament Building, Chicago (h-plate)	Mat footing section	-4,267	5,64x6,10	-3,35	279,14	35,4	43,2	59,8
20	Shanghai Theme Park (Block 1)	Vacuum pressure			-1,00	-69,37	69,2	55,0	58,2
21	Shanghai Theme Park (Block 2)	Vacuum pressure			-1,00	-69,37	64,5	55,0	61,1
22	Shanghai Theme Park (Block 7)	Vacuum pressure			-1,00	-53,07	57,0	50,0	54,3
23	Shanghai Theme Park (Block 8)	Vacuum pressure			-1,00	-80,00	83,5	85,0	88,7
24	Shanghai Theme Park (Block 9)	Vacuum pressure			-1,00	-79,45	93,3	90,0	97,4
25	Shanghai Theme Park (Block 10)	Vacuum pressure			-1,00	-80,00	83,5	85,0	92,8
26	Shanghai Theme Park (Block 19)	Vacuum pressure			-1,00	-63,06	83,7	70,0	78,5
27	Shanghai Theme Park (Block 20)	Vacuum pressure			-1,00	-75,52	90,3	80,0	88,7
28	Shanghai Theme Park (Block 21)	Vacuum pressure			-1,00	-57,21	77,1	65,0	73,3
29	Shanghai Theme Park (Block 22)	Vacuum pressure			-1,00	-69,37	61,2	55,0	61,4
30	Shanghai Theme Park (Block 23)	Vacuum pressure			-1,00	-60,80	59,6	50,0	57,2
31	Shanghai theme park (Block 32)	Vacuum pressure			-1,00	-60,24	58,6	55,0	59,8
32	Trial embankment, Malaysia	Embankment	3 m high, 50 m x 32 m in plan		-1,50	61,50	187,0	159,5	188,0

The degrees of correlation, R^2, and degrees of determination, S_d, are as follows:

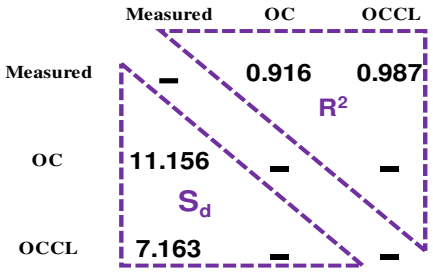

Figure 5. Correlation and determination coefficients, of the oedometric criterion and the oedometric continuous corrected law, with the settlement measurements of the 32 cases

These results demonstrate the good fit of the oedometric continuous corrected law with the measured settlements, significantly exceeding the fit obtained using the simple oedometric criterion, reducing the degree of determination by 36% and increasing the degree of correlation with the measured values.

This new procedure is limited to the application in settlement estimation in cases of shallow foundations, subjected to increasing vertical loads, and that the stress state must be equal or close to that of radial symmetry for horizontal stresses.

5 CONCLUSIONS

The oedometric continuous corrected law superimposes the horizontal deformations effect on the vertical oedometric deformation and allows effective analysis of settlement estimates on shallow foundations. According to the analysis of 32 measured settlement cases, this new law presented an 101,4% average accuracy with respect to the measured settlements, surpassing the precision using the oedometric criterion.

6 REFERENCES

Balasubramaniam, A. S., Cai, H., Zhu, D., Surarak, C., & Oh, E. Y. N. (2010). Settlements of embankments in soft soils. *Geotechnical Engineering*, *41*(2). http://hdl.handle.net/10072/40431

Balasubramaniam, A. S., Huang, M., Bolton, M., Oh, E. Y. N., Bergado, D. T., & Phienwej, N. (2007). Interpretation and Analysis of Test Embankments in Soft Clays with and without Ground Improvement. *Proceedings of the Sixteenth Southeast Asian Geotechnical Conference*, *January*, 1–18. http://hdl.handle.net/10072/16582

Briaud, J. L., & Gibbens, R. (1997). Large-scale load test and data base of spread footings on sand. In *FHWA-RD-97-0688*.

Briaud, J. L., & Gibbens, R. (1999). Behavior of Five Large Spread Footings in Sand. *Journal of Geotechnical and Geoenvironmental Engineering*, *125*(9), 787–796. https://doi.org/10.1061/(ASCE)1090-0241(1999)125:9(787)

Chen, L., Gao, Y., Elsayed, A., & Yang, X. (2019). Soil Consolidation and Vacuum Pressure Distribution Under Prefabricated Vertical Drains. *Geotechnical and Geological Engineering*, *37*(4), 3037–3048. https://doi.org/10.1007/s10706-019-00822-3

Da Fonseca, A. V., Fernandes, M. M., & Cardoso, A. S. (1997). Interpretation of a footing load test on a saprolitic soil from granite. *Geotechnique*, *47*(3), 633–651. https://doi.org/10.1680/geot.1997.47.3.633

Eggestad, A. (1964). Deformation measurements below a model footing on the surface of dry sand. *Norwegian Geotechnical Institute Publication*, *58*, 29–35.

Indraratna, B., Zhong, R., Fox, P. J., & Rujikiatkamjorn, C. (2017). Large-Strain Vacuum-Assisted Consolidation with Non-Darcian Radial Flow Incorporating Varying Permeability and Compressibility. *Journal of Geotechnical and Geoenvironmental Engineering*, *143*(1), 04016088. https://doi.org/10.1061/(asce)gt.1943-5606.0001599

Janbu, N. (1963). Soil compressibility as determined by oedometer and triaxial tests. *Proceeding of the European Conference on Soil Mechanics and Founation Engineering*, *1*, 245–251.

Lambe, T. W., & Marr, W. A. (1979). Stress path method: Second ed. *ASCE J Geotech Eng Div*, *105*(6), 727–738. https://doi.org/10.1061/ajgeb6.0000821

Loganathan, N., Balasubramaniam, A. S., & Bergado, D. T. (1993). Deformation analysis of embankments. *Journal of Geotechnical Engineering*, *119*(8), 1185–1206. https://doi.org/10.1061/(ASCE)0733-9410(1993)119:8(1185)

Mesri, G., & Choi, Y. K. (1985). Settlement analysis of embankments on soft clays. *Journal of Geotechnical Engineering*, *111*(4), 441–464. https://doi.org/10.1061/(ASCE)0733-9410(1985)111:4(441)

Naime, W. (2019). Ley Edométrica-Continua para el comportamiento esfuerzo-deformaciónón de los suelos. *Revista de La Facultad de IngenieríaUCV*, *34*(3). http://saber.ucv.ve/ojs/index.php/rev_fiucv/article/view/20078

Naime, W. (2022). Oedometric-continuous corrected law for the stress-strain relationship of soils under shallow foundations. In Prof. Md Mizanur Rahman and Prof. Mark Jaksa (Ed.), *Proceedings of 20th International Conference on Soil Mechanics and Geotechnical Engineering* (pp. 871–876).

Naime, W., & Gavidia, A. (2022a). Definición de zonas de falla en suelos debajo de fundaciones superficiales con base en la ley edométrica continua corregida continua corregida. *Boletín de La Academia Nacional de La Ingeniería y El Hábitat*, *54*, 83 – 91. http://www.acading.org.ve/info/publicaciones/boletines/boletin54.php

Naime, W., & Gavidia, A. (2022b). Estimación de desplazamientos horizontales y deformaciones unitarias en el suelo debajo de fundaciones superficiales con base en la ley edométrica continua corregida. *Boletín de La Academia Nacional de La Igeniería y El Hábitat*, *54*, 75–82. http://www.acading.org.ve/info/publicaciones/boletines/pubdocs/BOLETIN_54.pdf

Ohde, J. (1939). Zur Theorie der Druckverteilung im Baugrund. *Der Bauingenieur*, *20*, 451–459.

Papadopoulos, B. P. (1992). Settlements of shallow foundations on cohesionless soils. *Journal of Geotechnical Engineering*, *118*(3), 377–393. https://doi.org/10.1061/(ASCE)0733-9410(1992)118:3(377)

Peck, R. B. (1955). Observed and computed settlements of structures in Chicago. *Engineering Experiment Station Bulletin No 429*, *52*(53), 60.

Skempton, A. W., Peck, R. B., & Macdonald, D. H. (1955). Settlement analyses of six structures in chicago and london. *Proceedings of the Institution of Civil Engineers*, *4*(4), 525–542. https://doi.org/10.1680/iicep.1955.11401

Sridharan, A., & Gurtug, Y. (2005). Compressibility characteristics of soils. *Geotechnical and Geological Engineering*, *23*(5), 615–634. https://doi.org/10.1007/s10706-004-9112-2

Stamatopoulos, A., & Kotzias, P. (1974). The specific constrained modulus. *Eighth International Conference of Soil Mechanics and Foundations Engineering*, 397–402.

Stamatopoulos, A., & Kotzias, P. C. (1978). Soil Compressibility as Measured in the Oedometer. *Geotechnique*, *28*(4), 363–375. https://doi.org/10.1680/geot.1978.28.4.363

Wijemunige, p, & Moh, Z. C. (1989). Trial embankment with stage loading and vertical drains. *Proc., Int. Symp. on Trial Embankments on Malaysian Marine Clays*, *2*, 26/1–26/11. http://www.maaconsultants.com/common/publications/1986/1986-033.pdf

Wissa, A. E. Z., Christian, J. T., Davis, E. H., & Heiberg, S. (1971). Consolidation at constant rate of strain. *ASCE J Soil Mech Found Div*, *97*(SM10). https://doi.org/10.1061/jsfeaq.0001999

Yune, C.-Y., & Olgun, G. (2016). Effect of Layering on Total Consolidation Settlement of Normally Consolidated Clay in 1D Conditions. *Journal of Geotechnical and Geoenvironmental Engineering*, *142*(2), 06015015. https://doi.org/10.1061/(asce)gt.1943-5606.0001415